

THE PHYSICAL REVIEW

A journal of experimental and theoretical physics established by E. L. Nichols in 1893

SECOND SERIES, VOL. 128, No. 2

OCTOBER 15, 1962

Electrohydrodynamics of Superfluid Helium in Narrow Channels*

W. JIM NEIDHARDT† AND JACK FAJANS
Stevens Institute of Technology, Hoboken, New Jersey
(Received June 8, 1962)

The flow of superfluid helium from a liquid reservoir to vacuum through a 10^{-6} cm channel, which was enhanced tenfold by an electric field of 3×10^6 V/cm when a phase boundary occurred within the channel, was unaffected when the boundary moved past the channel and field. Superfluid flow at subcritical velocity given by $\Gamma - \Gamma_0 = f(T)V^2$, when increased to critical flow under the influence of electrostrictive pressures was given by $\Gamma = [\rho_n/\rho][\eta(T_\lambda)/\eta(T)]K_n + [\rho_s/\rho]K_s$, with Γ and Γ_0 the flow with and without applied electric field, V the applied voltage, T the temperature, ρ_n and ρ_s the normal and superfluid densities, ρ the total density, η the viscosity, and K_n and K_s flows obtained from normalization of data. A coincidence was noted between a maximum at 2.08°K in the relative flow and an already reported maximum at 2.10°K in thermal boundary conduction. Any shift in the λ point induced by a macroscopic field of 1.5×10^6 V/cm was less than 0.02°K, but displacements as great as 0.5°K were induced by use of very fine channels.

INTRODUCTION

HELIUM transport under the influence of electric fields may appropriately be termed electrohydrodynamic in the instant investigation, since electrostrictive forces and forces derived from dielectric gradients substantially altered the field free flow pattern. The origin of the net electrostrictive forces and dielectric gradients was a liquid-vapor interface in the strong-field region of the narrow channels which were used.

A number of earlier related papers may be cited. The work of Giaque *et al.*¹ had characteristics similar to those of our field-free flow, and extensive work has been carried out on field-free flow with liquid-helium reservoirs at both ends of the channel (i.e., without an interior phase boundary).²⁻⁴

Dielectric breakdown at fields of 10^6 V/cm was es-

tablished by Blank and Edwards⁵ for stationary liquid helium between spherical electrodes 0.15 mm apart; nevertheless, in the present experiment fields of 3×10^6 V/cm were employed.

McCrum and Eisenstein⁶ have suggested that boundary fields alter the superfluid behavior of liquid helium in films and fine channels. The lowering of the λ -transition temperature in the flow of unsaturated superfluid film⁷ and of liquid in fine channels⁸ may be caused by intense electric fields at the liquid substratum boundary.

EXPERIMENT

The amount of helium flowing from a liquid reservoir through a superleak, Fig. 1, to an evacuated chamber at room temperature was obtained by measuring the collected gas. The flow channel was the space between the stainless steel and fluorlin arising from submicroscopic imperfections in the surfaces which persisted after compression of the assembly by a spring. A poten-

* This work was made possible through support provided by the Office of Scientific Research, U. S. Air Force, and the National Aeronautics and Space Administration.

† Present address: Newark College of Engineering, Newark, New Jersey.

¹ W. F. Giaque, J. W. Stout, and E. R. Barieau, *J. Am. Chem. Soc.* **61**, 654 (1939).

² J. F. Allen and A. D. Misener, *Proc. Roy. Soc. (London)* **A172**, 467 (1939).

³ R. Bowers and K. Mendelssohn, *Proc. Phys. Soc. (London)* **A63**, 178 (1950); *Proc. Roy. Soc. (London)* **A213**, 158 (1952).

⁴ K. R. Atkins, *Phil. Mag. Suppl.* **1**, 169 (1952).

⁵ C. Blank and M. H. Edwards, *Phys. Rev.* **119**, 50 (1960).

⁶ N. G. McCrum and J. C. Eisenstein, *Phys. Rev.* **99**, 1326 (1955).

⁷ E. Long and L. Meyer, *Phys. Rev.* **79**, 1031 (1950); **85**, 1030 (1952).

⁸ K. R. Atkins, H. Seki, and E. V. Condon, *Phys. Rev.* **102**, 582 (1956).

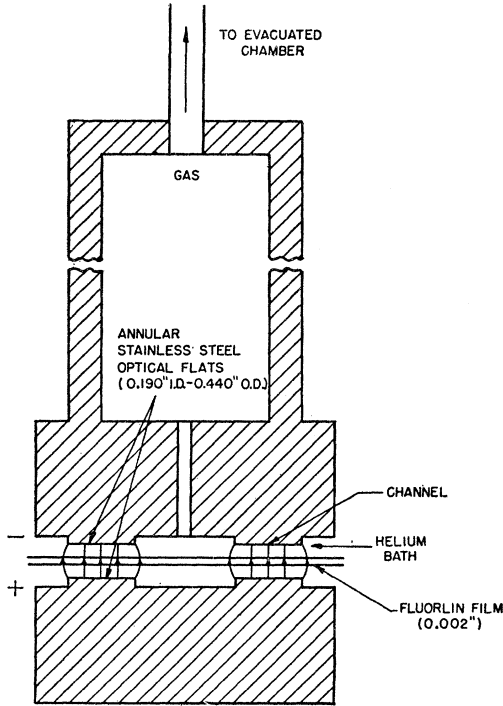


FIG. 1. Representation of components of flow channel before compression by a spring (not shown) to 600–950 psi. Electric field was confined substantially to the region designated. Flow occurred through a channel 10^{-5} cm thick between the fluorlin film and the stainless-steel surface.

tial difference of 0–8000 V dc applied across the fluorlin film between the annular optical flats produced fields up to 3×10^6 V/cm in the helium channel. The electrostatic attraction between the flats, which was usually less than 3% of the spring force and always less than 10% of it, affected the channel size slightly.

The flow rate Γ in atoms per second was computed from

$$\Gamma = (v/kT)(\Delta P/\Delta t), \quad (1)$$

where v , T , and $\Delta P/\Delta t$ were the volume, temperature, and rate of pressure rise of the collection chamber, and k is Boltzmann's constant. A macroscopic electric field E was computed from

$$E \approx (V/d)(\kappa_F/\kappa_H), \quad (2)$$

under the assumption that the fluorlin film thickness, $d = 5 \times 10^{-3}$ cm, was much greater than the helium channel thickness, 10^{-5} cm. V was the applied voltage, $\kappa_F = 2.0$ the dielectric constant of fluorlin, and $\kappa_H = 1.05$ the dielectric constant of liquid helium. The macroscopic field E was indicative of the microscopic fields in the channel.

Electrostriction

Following Stratton's⁹ presentation, the force per unit

volume exerted by an electric field on a dielectric fluid is

$$\mathbf{f} = -\frac{1}{2}\epsilon_0 E^2 \nabla \kappa + \frac{1}{2}\epsilon_0 \nabla (E^2 \tau d\kappa/d\tau), \quad (3)$$

where τ is the mass density. The first term is significant for an inhomogeneous dielectric; the second is referred to as the electrostriction term. Using the Clausius-Mossotti relationship

$$(\kappa - 1)/(\kappa + 2) = c\tau \quad (4)$$

to give the dependence of κ on τ , (3) becomes

$$\mathbf{f} = -\frac{1}{2}\epsilon_0 E^2 \nabla \kappa + \frac{1}{6}\epsilon_0 \nabla [E^2 (\kappa - 1)(\kappa + 2)]. \quad (5)$$

In equilibrium the electric body forces (5) acting on a fluid are related to the pressure gradient ∇P by

$$\nabla P = -\frac{1}{2}\epsilon_0 E^2 \nabla \kappa + \frac{1}{6}\epsilon_0 \nabla [E^2 (\kappa - 1)(\kappa + 2)]. \quad (6)$$

Figure 2(a) depicts helium flowing from a reservoir of liquid 1 through a channel of length l and thickness t to a region of vacuum 4. A liquid-gas interface demarcates the liquid 2 in the channel from the channel gas 3, and an electric field is applied along the entire channel length.

Integration of Eq. (6) leads to the equilibrium pressure distribution shown in Figs. 2(b) and 2(c). In Fig. 2(b) the effect of the electrostriction term is broken into three parts: $\Delta P_{12}^{(s)}$ the change at the channel entrance, $\Delta P_{23}^{(s)}$ the change at the interface, and $\Delta P_{34}^{(s)}$ the change at the exit. The effect of the $\nabla \kappa$ term at the interface is designated $\Delta P_{23}^{(\kappa)}$. $P_v + \Delta h$ gives the sum of vapor pressure and gravitational (hydrostatic) pressure, and $\Delta P' \approx \Delta P_{12}^{(s)}$.

In Fig. 2(c) the total pressure is plotted, and the slight dip shown at the interface is computed on the basis of constant field strength. In the actual experiment, the electric field in the gas channel was slightly greater than the field in the liquid channel with, correspondingly, a small increase in pressure at the interface. Figures 2(b)–(g) represent only the fluid pressure distribution and do not display electric or thermomechanical body forces.

For an applied potential difference of 4000 V which gave rise to a macroscopic field $E = 1.5 \times 10^6$ V/cm, $\Delta P_{12}^{(s)}$ was 36 mm Hg. The quantities $\Delta P_{23}^{(s)}$ and $\Delta P_{23}^{(\kappa)}$ were also approximately this size; the pressure dip at the interface in Fig. 2(c) is exaggerated.

Procedure

The pressure in the collection chamber, measured with an Alphatron gauge was plotted as a function of time for a given temperature and value of electric field, and the flow rate was determined from the slope in the linear region of this plot with Eq. (1). When the time interval of collection was sufficiently long, the pressure in the collection chamber reached a limiting value equal to the vapor pressure of the bath liquid for all electric fields and channel sizes.

⁹ J. A. Stratton, *Electromagnetic Theory* (McGraw-Hill Book Company, Inc., New York, 1941), pp. 137–151.

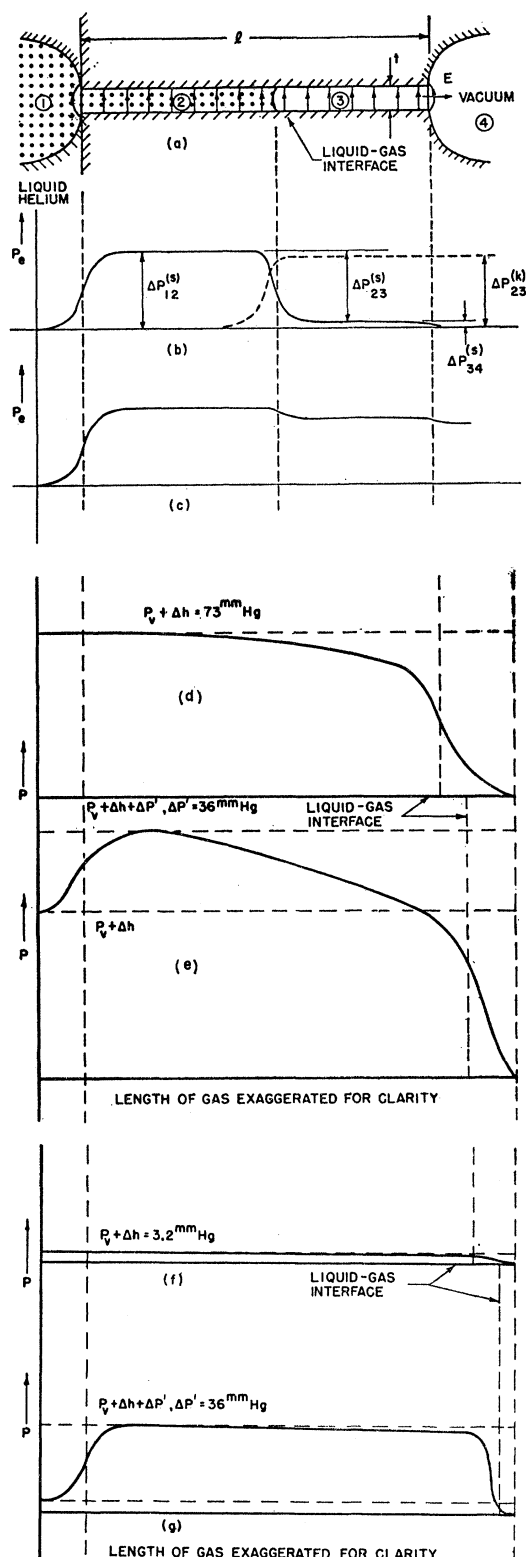


FIG. 2. Pressure distributions in channel with liquid-gas interface and macroscopic electric field. (a) Portrayal of channel; (b) components of equilibrium pressure induced by field; (c) total equilibrium pressure induced by field; (d) field-free pressure dis-

A typical flow measurement below the λ point required 13 min. During this interval the pressure in the collection chamber rose to 800μ Hg and the bath temperature was controlled to 0.002°K . Flow measurements at a given temperature and field were always repeated, and most measurements were taken in order of either ascending or descending temperature.

RESULTS

The channel thickness t for size A (discussed below) channels was estimated from measurements of air flow at $T=293^\circ\text{K}$. The linear rise of flow with pressure differential observed experimentally was indicative of Knudsen flow, and t was found to be 3×10^{-5} cm on the basis of flow between parallel planes.

From the data in the temperature range 4.2°K to the λ point another estimate of the channel thickness was made. The pressure distributions of Figs. 2(d) and 2(e) follow from the assumption of laminar liquid flow from the channel entrance to the interface and "slip" flow¹⁰ in the gas from the interface to the exit. The pressures at the interface were calculated for the temperature range from the various measured quantities—flow, entrance pressure, etc.—with an assumed value of channel thickness.

The most plausible set of interface pressures rather sharply defined 1.2×10^{-5} cm as the thickness of a size A channel. The pressure at the interface was lower than the bath vapor pressure because of the evaporative cooling at the interface as well as the dynamic or non-equilibrium flow condition. To the viscous loss in the field-free liquid flow was added essentially all of the electrostrictive pressure $\Delta P_{12}^{(s)}$ when the voltage was applied. The discrepancy between the two determinations of thickness was most likely due to the inadequacy of representing the channel as a pair of parallel planes.

Superfluid Flow

Classification of channel size by the magnitude of the flow rate as in Fig. 3 led to a rough correlation of flow characteristics with and without applied electric field. From the size of the largest class A (maximum $\Gamma_0 \approx 2 \times 10^{18}$) to the size of the smallest class D (maximum $\Gamma_0 \approx 0.3 \times 10^{18}$), the pressure exerted on the fluorlin film by the annular optical flats varied from 600 to 950 psi (Γ_0 was the field free flow).

The maximum in Γ , exemplified in Fig. 3, was most pronounced for channels with the largest flow rates. As the channel decreased in size the maximum appeared at lower temperatures; for the smallest channel size the maximum was not reached even at 1.30°K , the lowest temperature attained.

¹⁰ R. D. Present, *Kinetic Theory of Gases* (McGraw-Hill Book Company, Inc., New York, 1958), p. 63.

tribution in flowing normal fluid; (e) distribution in flowing normal fluid with 1.5×10^6 V/cm; (f) field-free distribution in flowing superfluid; (g) distribution in flowing superfluid with 1.5×10^6 V/cm.

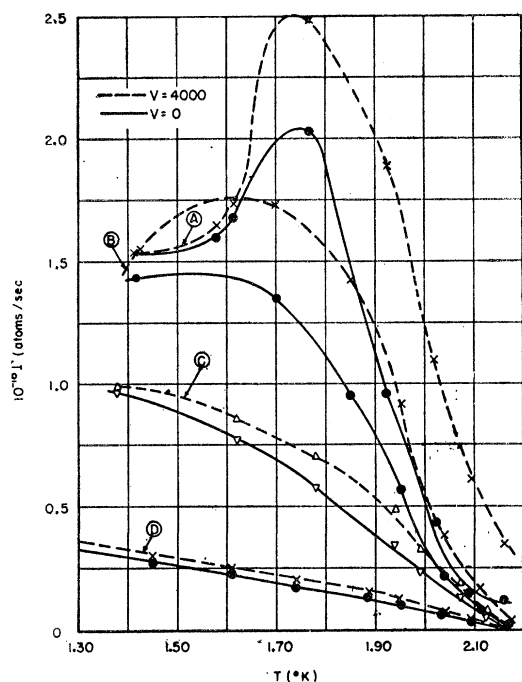


FIG. 3. Superfluid flow in channels of various sizes with and without field.

Figure 4 shows a maximum in the relative increase in flow rate $(\Gamma - \Gamma_0)/\Gamma_0$ for $V = 4000$ V near 2.08°K . The maximum appeared at this temperature for all applied voltages, Fig. 5, and was quite pronounced in the larger channel sizes. However, for channel size *D* it was not observed at any temperature. Perhaps by no more than a coincidence, a maximum in thermal conduction from a wall to superfluid has been noted at 2.1°K by White

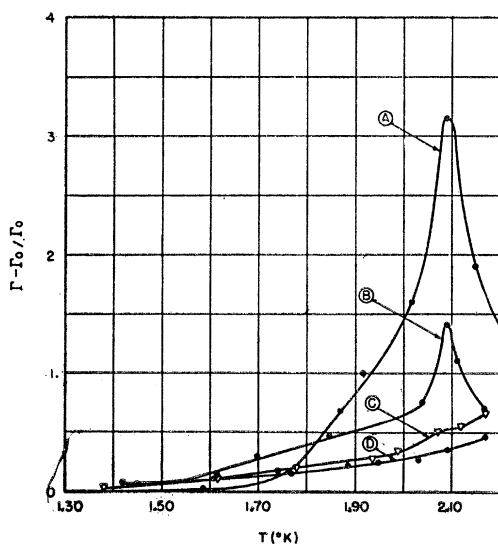


FIG. 4. Relative flow augmentation in channels of various sizes for field of 1.5×10^{-6} V/cm.

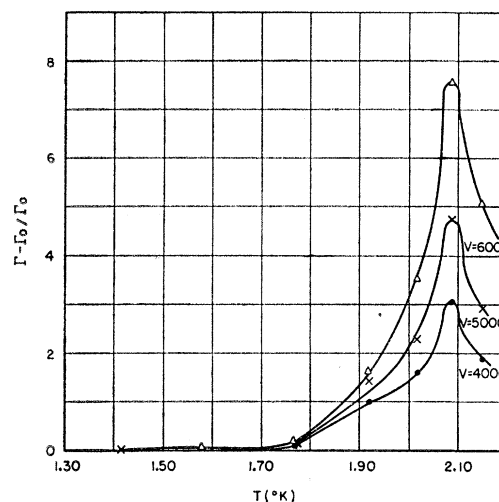


FIG. 5. Relative flow augmentation in a size *A* channel for various fields.

*et al.*¹¹ and by Andronikashvili and Mirskaia.¹² The flow was tenfold enhanced in some size *A* channels by a field of 3×10^6 V/cm.

Critical Velocity

The saturation values of Γ evident in the plots vs temperature and voltage presented in Figs. 6–8 are attributed to the superfluid's attainment of critical velocity¹³ at high fields. At low fields the superfluid velocity was subcritical. That the liquid-gas interface eventually reached the channel exit is attested to by the maxima of Fig. 6 and by the ineffectiveness of the field in the low-temperature region. The crossed curves of Fig. 8 also manifest this.

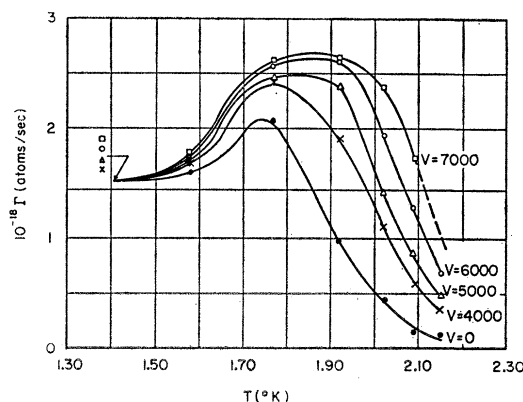


FIG. 6. Flow in an *A* channel for various fields.

¹¹ D. White, O. D. Gonzales, and H. L. Johnson, *Phys. Rev.* **89**, 593 (1953).

¹² E. L. Andronikashvili and G. G. Mirskaia, *J. Exptl. Theoret. Phys.* (U.S.S.R.) **29**, 490 (1955).

¹³ K. R. Atkins, *Liquid Helium* (Cambridge University Press, New York, 1959), pp. 88–91, 198–201.

Giauque, Stout, and Barieau¹ observed similar results for experiments where the entrance of a channel of width 10^{-4} cm was in liquid helium and the exit connected to an evacuated chamber. Their results, also, can be explained by assuming that at the lowest temperatures the liquid-gas interface moved past the exit of the channel thereby causing the flow rate to drop.

In the region of subcritical velocity $\Gamma - \Gamma_0$ was found to be proportional to V^n , where $n = 2.0 \pm 0.5$ (with extreme variation in n given). Figure 9 shows a log plot for a run representative of channel size A . No correlation between n and channel size was found. Each size, possessed high and low values of n , although n was constant during the run of any particular day.

Below the λ point the large rise in flow at zero field with decreasing temperature was due to the superfluid contribution to liquid flow. If it had been flowing at

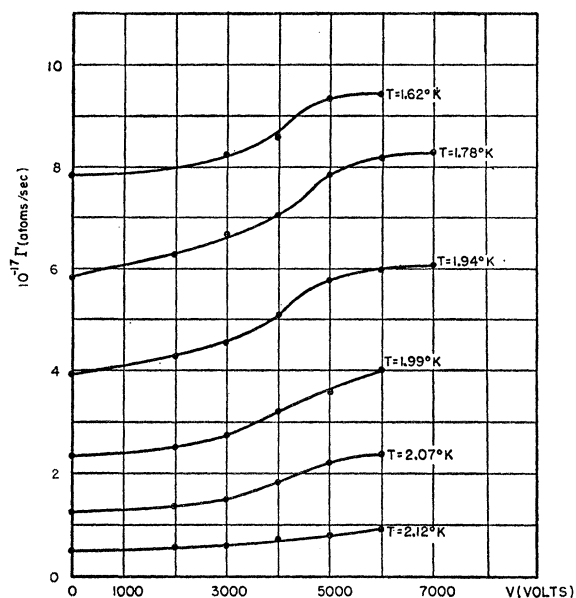


FIG. 7. Flow in a C channel for various temperatures.

critical velocity which is almost independent of temperature, the resulting flow rate would have been given by

$$\Gamma = (\rho_s/\rho)(L/M)\rho A u_c, \quad (7)$$

where A is the cross-sectional area of the channel, L is Avogadro's number, M is the gram atomic weight of helium, u_c is the critical velocity, ρ_s is the superfluid density, and ρ is the density.

Actually, Γ increased more slowly than ρ_s/ρ with decreasing temperature, indicating that the superfluid was flowing below critical velocity. This smaller flow may be attributed to the retarding thermomechanical¹⁴ pressure, which arose from the temperature differential created by the evaporation of liquid inside the channel.

¹⁴ Fritz London, *Superfluids* (John Wiley & Sons, Inc., New York, 1954), Vol. II, p. 70.

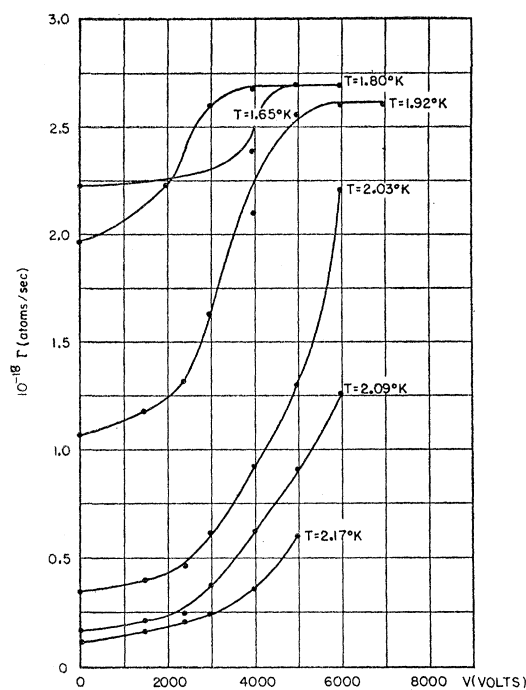


FIG. 8. Flow in an A channel for various temperatures.

The magnitude of this pressure was

$$\Delta P = \rho S \Delta T, \quad (8)$$

where S is the entropy per gram, ΔP was the pressure

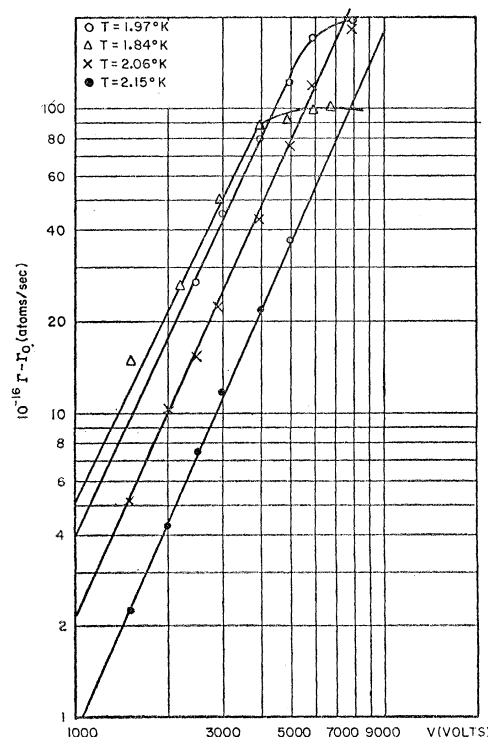


FIG. 9. Flow in an A channel for various temperatures.

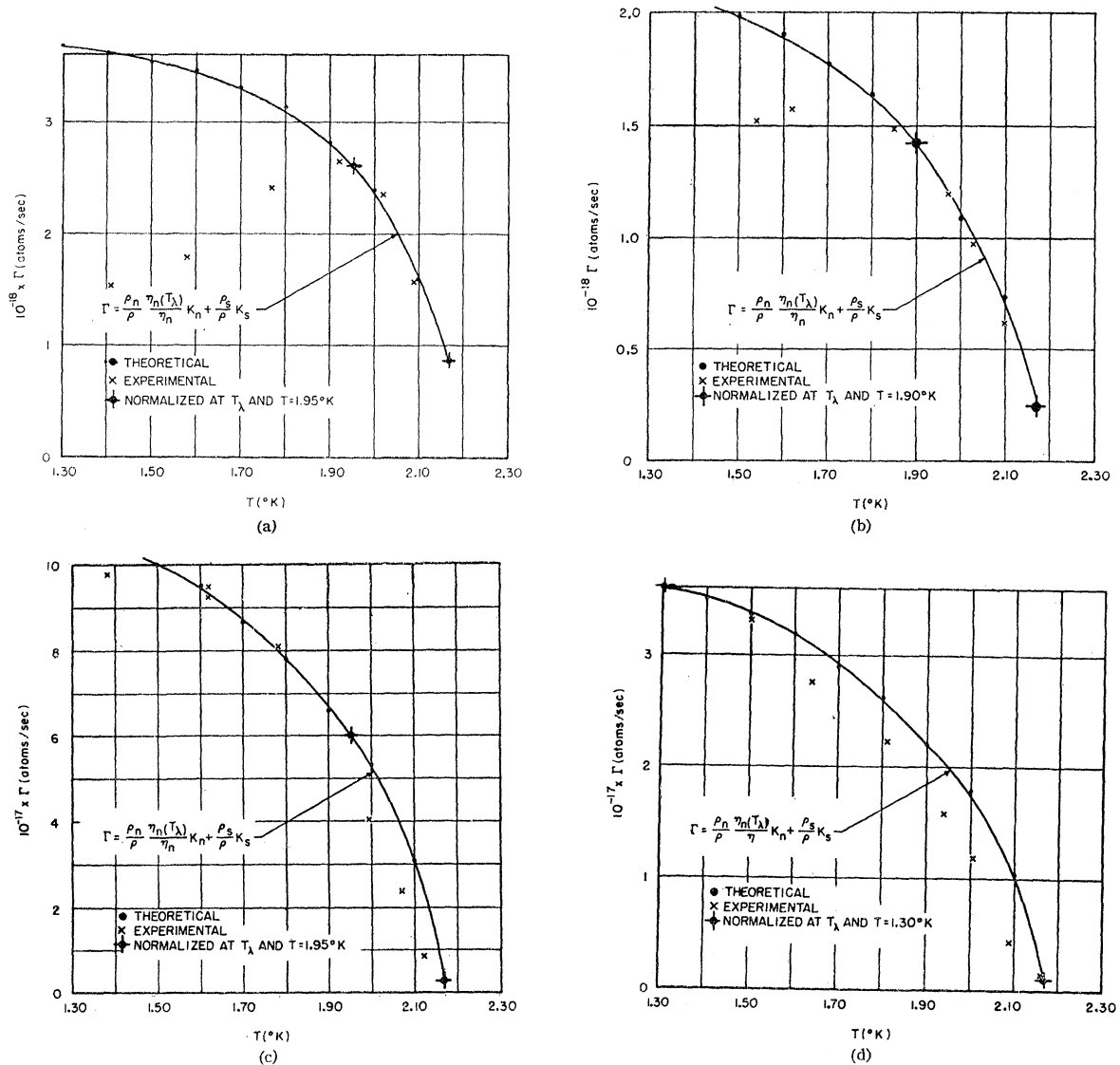


FIG. 10. Critical flow in channels of various sizes. (a) Size A channel at 3.0×10^6 V/cm; (b) Size B channel at 2.5×10^6 V/cm; (c) Size C channel at 2.0×10^6 V/cm; (d) Size D channel at 1.5×10^6 V/cm.

difference in the liquid between the entrance of the channel and the liquid-gas interface, and ΔT was the temperature difference between the bath fluid and the liquid-gas interface.

The thermomechanical pressure prevented the superfluid from penetrating the entire channel and flowing past the exit. The length of channel occupied by gas and the pressure drop in the gas were appropriate for the flow rate. The field induced flow was a second stronger indication that the penetration of the entire channel expected from the absence of superfluid viscosity and the net pressure acting on the liquid did not occur.

Inferences from the Occurrence of an Internal Interface

A flow increase proportional to the square of the electric field was deduced from the occurrence within the

channel of the liquid-gas interface. The additional thermomechanical pressure, $\Delta P'$, necessary to counteract the electric pressure [cf. Fig. 2(g)] acting on the liquid resulted from the cooling of increased evaporation. From an assumption that the additional field-induced temperature difference $\Delta T'$ between the bath and the liquid-gas interface was given in analogy with (8) by

$$\rho S \Delta T' = \Delta P' \approx \Delta P_{12}^{(s)} \quad (9)$$

an additional proportional amount of heat flow to the liquid in the channel was associated with $\Delta P_{12}^{(s)}$. The rate of helium evaporation or the net mass flow was proportional to the heat flow to the liquid in the channel. Thus, $\Delta P_{12}^{(s)}$, which was proportional to E^2 , caused the temperature difference between the liquid-gas interface

and the bath to increase by $\Delta T'$ with a proportional increase in mass flow.

Figures 2(f) and 2(g) show flow behavior at $T = 1.4^\circ\text{K}$, where only an 8% concentration of normal fluid was present to create liquid losses. When a voltage was applied electrostriction caused a sharp rise in pressure near the channel entrance. The pressure barely changed over most of the liquid region since no losses occurred in the superfluid flow and the amount of normal fluid present was small. Near the liquid-gas interface a sharp drop in pressure was closely compensated by a thermomechanical pressure gradient.

In recapitulation, from the observation that the liquid did not penetrate the entire channel it was argued that an electrostrictive pressure proportional to V^2 induced a commensurate augmentation of the flow rate. The deduction was in accord with the second observation that

$$\Gamma - \Gamma_0 = f(T)V^2 \quad (10)$$

below the λ point. Further, at high values of electric field the flow remained constant, the superfluid then being driven at critical velocity.

In Figs. 10(a)–(d) some conjectured curves of Γ vs T at the highest values of applied field have been plotted which follow from these presumptions:

(a) The highest field drove the superfluid to critical velocity and the flow of superfluid was governed by

$$\Gamma_s = (L/M)(\rho_s/\rho)\rho A u_c = (\rho_s/\rho)K_s, \quad (11)$$

with the critical velocity assumed independent of temperature.

(b) The flow of normal fluid was proportional to the normal fluid density, inversely proportional to the viscosity η , and given by

$$\Gamma_n = (\rho_n/\rho)[\eta(T_\lambda)/\eta(T)]K_n, \quad (12)$$

with variable pressure drop and length of liquid in the channel neglected.

From (11) and (12) the theoretical curve became

$$\Gamma = \Gamma_n + \Gamma_s = (\rho_n/\rho)[\eta(T_\lambda)/\eta(T)]K_n + (\rho_s/\rho)K_s. \quad (13)$$

K_n and K_s were determined for a particular channel by normalizing from two points on the experimental curve. For channel sizes A and B a good fit was obtained between T_λ and 1.90°K where Γ began to decrease, i.e., where the liquid had reached the channel exit.

In channel size C the theoretical curve agreed with experiment in the temperature range 1.95 to 1.60°K . The applied field was smaller than for channel sizes A and B and was not driving superfluid to the critical velocity over the whole temperature range. In channel size D experimental points fell below the theoretical ones in the temperature range 1.30°K to T_λ . The applied field, which was smaller still, was insufficient to drive the superfluid to critical velocity (field was limited by dielectric breakdown).

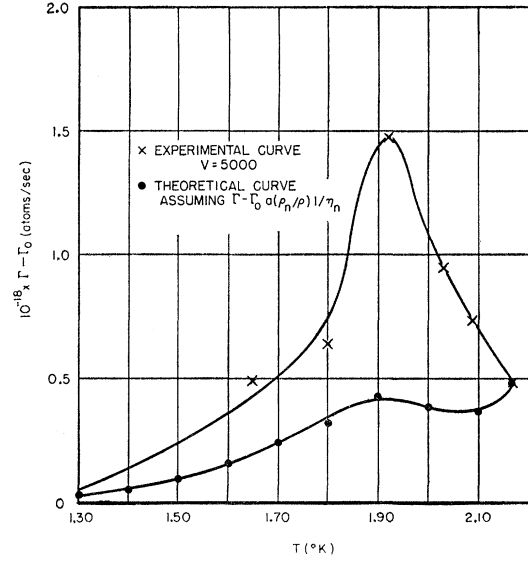


FIG. 11. Field-induced flow augmentation compared with conjectured normal fluid flow increase.

K_s , determined from the experimental data, made possible the calculation of the critical velocity. From experimental data for channel size A , K_s was found to be 3.8×10^{18} atoms/sec and u_c to equal 7 cm/sec with the channel thickness taken as 1.0×10^{-5} cm. Atkins⁴ reported the critical velocity of superfluid helium in a powder packed channel to vary from 13 to 3 cm/sec as channel size varied from 10^{-5} to 4×10^{-4} cm.

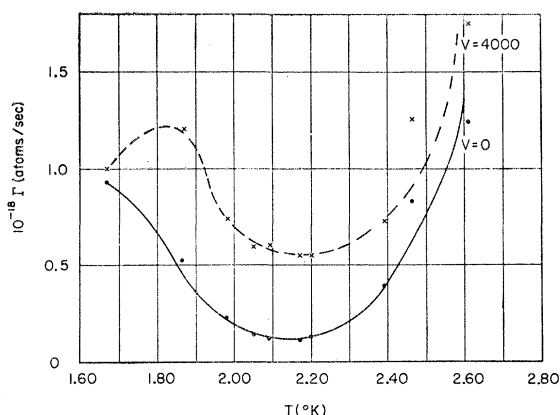
That the electric pressures affected both the normal fluid and the superfluid may be seen in another way. If the field had affected only the normal fluid, $\Gamma - \Gamma_0$ would have been proportional to $(\rho_n/\rho\eta)V^2$. For a leak representative of channel size A Fig. 11 compares this function with flow increment at fixed voltage, with the value of $\Gamma - \Gamma_0$ at the λ point used as a reference. The surmised increase in flow of the normal fluid could not alone account for the actual one.

Displacement of the Transition Point

Experiments with an applied field of 1.5×10^6 V/cm ($V = 4000$ V) to determine whether the λ point was shifted by electric field, are typified by the data of Fig. 12. A diffuse λ transition is indicated in the flow rates with and without field. From the data for various channel sizes, some showing the transition more sharply, it was concluded that a field of 1.5×10^6 V/cm shifted the λ point less than 0.02°K . Interpretation of the data was complicated by the interface temperature, which was several hundredths of a degree below the bath temperature and depended on the applied field strength.

Anomalous Flow Behavior

In a group of channels smaller than class D no flow was observed as the liquid-helium bath was initially

FIG. 12. Flow near the λ point in an A channel.

cooled from 4.2°K to a temperature below the λ point. After the sudden onset of flow at a temperature which ranged from 1.9 to 1.7°K , a normal pattern was observed throughout the entire temperature range. That is, flow

occurred above the λ point and increased sharply below it.

Summary

In addition to the pressure gradients, gravitational forces, and thermomechanical forces ordinarily encountered in liquid-helium hydrodynamics, body forces of electrostrictive origin were present and dominant in this work. Superfluid flow at less than critical velocity was brought to flow at critical velocity, as long as part of the flow channel was filled with gas, by electric pressures which affected both the normal and superfluid components of the liquid. The apparatus may be considered to be an electrohydrodynamic flow regulator.

ACKNOWLEDGMENTS

Discussions of many aspects of the research with Professor H. W. Meissner, Professor F. Pollock, and Professor S. I. Rubinow were of substantial value. The authors wish to note, also, the assistance of W. Steinert in the construction of the apparatus.

Film Flow of Liquid Helium at Low-Pressure Heads*†

H. SEKI‡

Department of Physics, University of Pennsylvania, Philadelphia, Pennsylvania

(Received May 8, 1962)

A steady-state method was developed and used to measure the flow rate of saturated liquid-helium films at small pressure heads. In this method a steady heat input into a glass vessel partially immersed in liquid helium generates the film flow inwards. A steady state is established when the rate of film flow is equal to the rate of distillation out of the vessel. The flow rate was derived from the temperature difference and level difference between the liquid in the vessel and the bath. Measurements in the vicinity of 1.2°K indicate a marked pressure-head dependence of the flow rate below a pressure head of 0.01 cm of liquid helium. A maximum flow rate for zero pressure head (± 0.001 cm of liquid helium) of about 5×10^{-6} cc/sec cm is observed. This rate is suggested to be the true critical flow rate of the film.

INTRODUCTION

ONE of the characteristic features of the superfluid flow of a saturated liquid-helium film is the relatively constant rate at which it flows regardless of the pressure head. This observation was one of the factors which led to the concept of critical velocity for the superfluid component in the two-fluid theory of liquid helium. The critical velocity is a velocity below which it is believed that the superfluid can flow with essentially no dissipation of its kinetic energy of flow. Such

a frictionless flow can occur with zero pressure head.¹

The observed flow rate of the helium film is usually expressed in cc/sec cm, so the average flow velocity is given by the quotient of the film-flow rate and the thickness of the film. However, the film thickness has been observed to vary with the height of the film above the bath, though the exact dependence of the thickness on the height is still open to debate. The interpretation of the flow rate is further complicated by the fact that the flow rate and thickness can be critically altered by condensation of small amounts of solid impurities and by the roughness of the substrate material. Con-

* This work has been submitted to the University of Pennsylvania in partial fulfillment of the requirements for the degree of Ph.D.

† This work was supported in part by the National Science Foundation.

‡ Present address: International Business Machines Corporation, Thomas J. Watson Research Center, Yorktown Heights, New York.

¹ Bibliography and better coverage may be found in the following review articles: (a) W. H. Keesom, *Helium* (Elsevier Publishing Company, Inc., Amsterdam, 1942). (b) R. G. Dingle, *Advances in Physics*, edited by N. F. Mott (Taylor and Francis, Ltd., London, 1952), Vol. 1, p. 111. (c) F. London, *Superfluids* (John Wiley & Sons, Inc., New York, 1954). (d) K. R. Atkins, *Liquid Helium* (Cambridge University Press, New York, 1959).